Design of Extremely Sensitive Refractive Index Sensors in Infrared for Blood Glucose Detection

Sandeep Kumar Chamoli, Subhash Chandra Singh, and Chunlei Guo

***Abstract*—Simple and easy to fabricate sensors with high sensitivity, high quality-factor (χ), large figure of merit (FOM), and narrow bandwidth are highly desirable for immediate point of care testing. In this article, we introduce a one-dimensional periodic array of barium flint glass on active plasmonic material, a thin gold film on silicon nitride (Si_3N_4) substrate. Reflection spectrum of the proposed structure exhibits a clear rejection of certain wavelength on normal incidence due to the coupling between incident plane wave and plasmonic wave. The effect of ambient refractive index or glucose concentration has been studied to measure the plasmonic sensitivity of the designed structure in blood glucose detection. After optimizing geometric parameters, the designed sensor achieved sensitivity and quality factor as high as ~ 2600 nm RIU^{-1} (refractive index unit) and ~1500 respectively. The calculated sensitivity, quality factor and FOM are much higher than the reported structures with a similar geometry in IR. Owing only one rejection band with narrow bandwidth, the designed structure can also be realized for optical filtering applications. Wide spectral tunability in the IR, close to 100 % peak absorbance and narrow bandwidth make the designed structures as an ideal candidate for surface-enhanced infrared absorption (SEIRA) spectroscopy.**

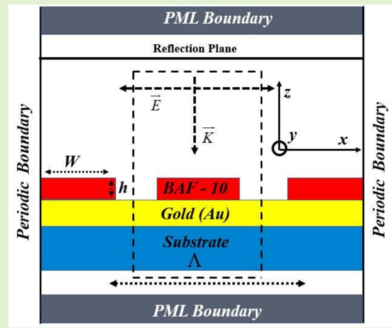

***Index Terms*— Surface plasmon resonance, optical sensors, optical filters, periodic structures, refractive index sensors, plasmonic sensors.**

I. Introduction

SURFACE plasmon polaritons (SPPs) are the excitation of electromagnetic (EM) waves propagating on the boundary between metal and air, and evanescently bound along the perpendicular direction [1]. Surface Plasmon Resonance (SPR) is a result of coupling between the incident electromagnetic field and the conduction electron at the dielectric-metal interface [2]. Prism and grating couplings are well known techniques to excite these surface plasmonic modes [2]–[4]. SPR properties of metals such as gold (Au), silver (Ag) and aluminum (Al) are widely explored to enhance performance of photonics and opto-electronic devices [5], waveguides and splitters [6], enhanced transmission [7], and optical sensors [5], [8]. Optical characteristics, such as permittivity of metal significantly affect the performance of grating based SPR sensors, so permittivity has a key role in designing SPR based refractive index sensors. Gratings made of Au, Ag and Al have their own advantage and limitation or drawbacks. Au has become frequently used SPR metal for refractive index sensor due to having high chemical stability. However, Al demonstrate narrower SPR reflection curve but with low chemical stability. To prevent oxidation of Al and Ag, Au can be used as a protective layer [9], [10]. The conventional approach of making optical filters and sensors is thin film based multi-layered structure. Recently, sub-wavelength grating structures that utilize the properties of surface resonance mode, such as guided-mode-resonance (GMR), are widely used for plasmonic sensing and filter applications [9]–[15]. In order to achieve narrow bandwidth in sub-wavelength grating structures, it is necessary to excite GMR modes along the length of the substrate on which the grating structure is formed [16]–[19]. Although sub wavelength grating filters suffer from multiple rejection bands in the transmission and reflection spectrum, plasmonic metallic structures also have

Manuscript received December 7, 2019; revised December 30, 2019; accepted December 31, 2019. Date of publication January 7, 2020; date of current version April 3, 2020. This work was supported in part by the National Key R&D Program of China under Grant 2017YFB1104700, in part by the National Natural Science Foundation of China under Grant 11674178, in part by the Jilin Provincial Science and Technology Development Project under Grant 20180414019GH, and in part by the Bill & Melinda Gates Foundation under Grant OPP1119542. The work of Sandeep Kumar Chamoli was supported by the CAS-TWAS Presidential's Fellowship. The associate editor coordinating the review of this article and approving it for publication was Dr. Carlos Marques. *(Corresponding authors: Subhash Chandra Singh; Chunlei Guo.)*

Sandeep Kumar Chamoli is with the Guo China-US Joint Photonics Laboratory, Changchun Institute of Optics, Fine Mechanics and Physics, Chinese Academy of Sciences, Changchun 130033, China.

Subhash Chandra Singh and Chunlei Guo are with the Guo China-US Joint Photonics Laboratory, Changchun Institute of Optics, Fine Mechanics and Physics, Chinese Academy of Sciences, Changchun 130033, China, and also with The Institute of Optics, University of Rochester, Rochester, NY 14627 USA (e-mail: ssingh49@ur.rochester.edu; guo@optics.rochester.edu).

Digital Object Identifier 10.1109/JSEN.2020.2964715

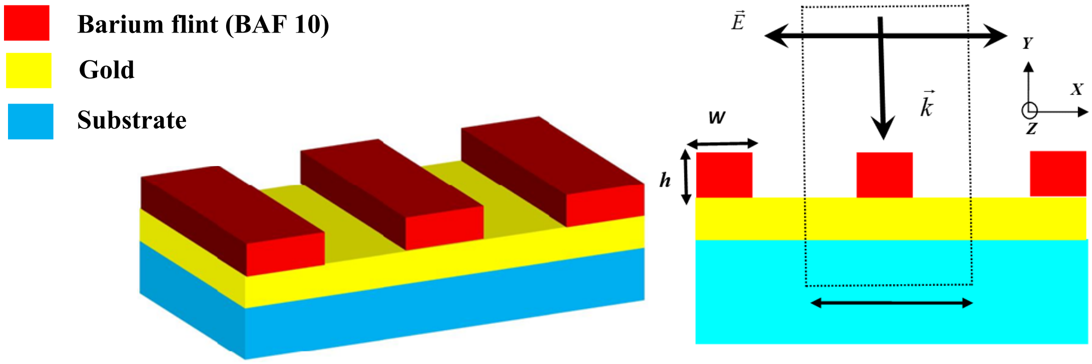

Fig. 1. (a) Perspective view; (b) Schematic of proposed sub wavelength grating simulation setup and geometry. Parameters used are grating thickness h, grating width W and grating period Λ. The dashed lines represent a unit cell of the periodic structure, enclosing the grating in the middle. The incident wave is travelling in the negative y direction. Electric field oscillations are in x direction.

the same issue. Additionally, metallic grating based plasmonic filters and sensors have wide bandwidth due to high optical absorption in metals in visible spectral region.

In general, the performance of any sensor is evaluated by its sensitivity, quality factor and figure-of-merit (FOM), and a higher quality factor is related to higher sensitivity and ultimately higher wavelength resolution. A wide range of plasmonic materials have been used in optical sensing applications [20]–[29]. Zhengqi *et al.* proposed a multispectral ultra-narrow band absorber based optical sensor with high sensitivity of 1000 nm/RIU, but very low, only 5, value of FOM [27]. Liu *et al.* suggested a refractive index sensor based on network type metasurface with FOM of ∼ 68.57 [28]. The metal-metal-dielectric-metal (MMDM) structure proposed by Luo *et al.* demonstrated FOM as high as 1054 [25]. To further enhance the sensitivity of plasmonic sensing devices, many geometrical structures, including nanorings [30], nanodisks [31], [32], and nanorods [33], are proposed. Shen *et al.* proposed a structure based on gold mushroom arrays with 10nm bandwidth and FOM of 108 [34]. A nanoslit microcavity based design, reported by Lu et al., is able to achieve bandwidth of 8nm [35]. Due to their relatively complex geometry, and low performance metrices, proposed sensor designs are time consuming and costly to fabricate using available fabrication techniques. The design of easy to fabricable plasmonic sensor structure with high performance metrices is highly desirable for the development of cost-effective sensing devices for immediate point-of-care in developing countries.

Performance of plasmonic sensors in the UV-visible region get hindered by high intrinsic optical absorption of the materials in that spectral region. On the other hand, most of the target biomolecules such as DNA and proteins do not absorb in the visible region but have strong vibrational and rotational transitions associated absorption in the infrared [34], [35]. However, resonance in the IR is wider and weaker as compared to that in UV-visible spectral region due to the underlying quantum mechanical limitations. Therefore, realizing narrow bandwidth plasmonic resonance in infrared and hence designing high performance refractive index sensors is challenging. In this paper, we report the design of a 1-D grating plasmonic sensor with high responsivity for glucose detection in the infrared region. We used barium flint glass, as grating material, on thin gold film deposited on silicon nitride substrate to design a novel plasmonic sensor. The calculated sensitivity for the designed sensor is around 2600 nm/RIU with quality factor as high as 1500. The narrow bandwidth and strong absorption at resonance make the designed structure very reliable for plasmonic sensing applications. Moreover, the proposed structure is easy to fabricate. The designed structure enables only one narrow bandwidth (2.5 nm) rejection band that can be also used for filtering applications. Wide spectral tunability in the infrared, close to 100 % peak absorbance and narrow bandwidth make the designed structures as an ideal candidate for surface-enhanced infrared absorption (SEIRA) spectroscopy [36]. By spectral tuning and overlapping the resonance of designed plasmonic structure with a specific absorption band of target biomolecule in IR, a selective vibrational mode can be excited to achieve large signal from ultra-small volume. The proposed structure can be used for the fabrication of ultra-narrow band rejection filter, SEIRA substrates, and plasmonic sensors, and can be extended to other spectral regions.

II. Device Structure and Simulation Parameters

Figure 1 (a) and (b) demonstrate the design of a 1-D grating structure made of barium flint (BAF 10) on gold (Au) thin film as an active plasmonic metal on Si_3N_4 substrate. The structural parameters, such as period of grating (Λ), grating height (h), and grating width (W) were swept to design a highly responsive plasmonic sensor. A finite difference time domain (FDTD) method created by Yee and developed by lumerical Solution Inc. is used for the simulation of proposed sub wavelength grating structure [36]. The Lorentz-Drude's material model was used to calculate the optical constants of Au [37]. The refractive index of BAF – 10 is calculated using following expression:

$$n^2 - 1 = \frac{1.5851495\lambda^2}{\lambda^2 - 0.00926681282} + \frac{0.143559385\lambda^2}{\lambda^2 - 0.0424489805} + \frac{1.08521269\lambda^2}{\lambda^2 - 105.613573} \quad (1)$$

The Perfectly Matched Layer (PML) boundary conditions are used in the Y-direction while periodic boundary conditions are used in the X-direction.

A 2-D simulation has been used to estimate the electric field distribution and optical response in the grating structure. The light incidents normally on the structure and allowed to propagate in the Y-direction with electric field oscillation along the X-direction. The grating is infinitely extended in the Z-direction, therefore plasmonic modes cannot be observe for Z-polarized wave. To simulate optical reflection data of the structure, an optical power monitor is placed in between the source and upper PML boundary.

An electromagnetic (EM) wave incident on the 1D periodic grating structure at a given incident angle excites the surface plasmon wave. The wave vector that corresponds to the surface plasmon and the phase matching condition is given by the following formula [1].

$$k_{sp} = k_0\sqrt{\frac{n_1^2}{n_1^2+\varepsilon_m}} \tag{2}$$

where $k_0 = \frac{2\pi}{\lambda_0}$, k_0 represents the wave vector in free space, n_1 is refractive index of incidence medium, and ε_m is the permittivity of metal with m an integer.

$$k_0 n_1 \sin\theta_{inc} + m\frac{2\pi}{\Lambda} = \pm\left\{k_0\sqrt{\frac{n_1^2\varepsilon_m}{n_1^2+\varepsilon_m}}\right\} \tag{3}$$

Equation (3) is known as phase matching condition. For a given incidence angle θ_{inc}, the wavelength that satisfies the phase matching condition is known as resonance wavelength λ_0 Similarly, for a given wavelength, λ the incident angle that satisfies phase matching condition is termed as θ_{sp}. From equation 2, one can see that refractive index, n_1, of the medium can control phase matching condition and hence it can tune resonance wavelength (λ_0) and resonance angle ($\theta_{inc} = \theta_{sp}$) for a given plasmonic structure. This dependence of λ_0 and θ_{sp} on refractive index of the ambient can be utilized in refractive index sensors for analyte detection. Generally, the response of such a sensor is determined by measuring the variation in the specular reflectance at a given wavelength. The characteristics of such a sensor rely on the resonance wavelength, angle of incidence, and FWHM of resonance peak. Sensitivity of refractive index sensor can be defined as follows:

$$S = \frac{\Delta\theta_{sp}}{\Delta n_1} \quad \text{or} \quad S = \frac{\Delta\lambda_0}{\Delta n_1} \tag{4}$$

where $\Delta\theta_{sp}$ and $\Delta\lambda_0$ are the shift in resonance angle and resonance wavelength respectively corresponding to change in the refractive index Δn_1 of ambient. For a high sensing performance, high sensitivity and narrow bandwidth are required to detect the small variation in the ambient refractive index. Eventually the performance of a refractive index sensor can be defined using its quality factor (χ) and Figure-of-merit (FOM), where these performance metrices depend on the sensitivity, FWHM and dip strength as follows:

$$\chi = \frac{Sensitivity}{FWHM} \tag{5}$$

$$FOM = \frac{Dipstrength}{FWHM} \tag{6}$$

here, we studied reflection from plasmonic structure for a normal incidence light in the wavelength range from 1000 to 2000 nm. For the optimization of geometric parameters of plasmonic structure, water (n = 1.33) was first used as ambient medium. Later, optimized plasmonic structure was used for numerical detection of glucose concentration in water. For this purpose, the refractive index of the medium was numerically varied from 1.33 to 1.38 to simulated concentration of glucose from 0 g/100 ml (pure water) to 30 g/100 ml. The maximum calculated FOM and quality factor for the designed plasmonic structure are 0.38 and 1500, respectively. All the simulation has been done using one-unit cell of the structure.

III. Results and Discussions

A. Equations Numerical Optimization for Geometric Parameters of Plasmonic Grating

We numerically simulated spectral reflectance from designed plasmonic 1D grating by sweeping its different geometric parameters such as grating width (W), grating height (t), and grating period (Λ). First, we swept grating width W in the range of 300-900 nm with the step of 300 nm by keeping grating period (Λ = 1064 nm) and grating thickness (t = 125 nm) constant.It is interesting to note that dip strength (peak absorbance) increases by increasing grating width from 300 to 600 nm with strong red shift in the resonance peak position. However, further increase in the grating width to 900 nm, results decrease in dip-strength with longer wavelength shift in the resonance wavelength. Fig 2 (b) demonstrates a 2 D plot between reflectance and wavelength for different grating width. Strong absorption peak is due to coupling between surface plasmon mode and incident EM wave. A clear red shift in the resonance wavelength can be seen with increasing grating width due to red shift in surface plasmon mode. Since a minimum FWHM and maximum absorbance correspond to the W = 300 nm, therefore we used this grating width as a fixed parameter during further optimization of other geometric parameters. To further optimize the structure, we next study the variation in resonance peak position and peak width with varying grating thickness. Figures 2 (c) and (d) demonstrate line and 2D plots for variation in spectral absorbance with grating thickness. We swept grating thickness in the range of 10-200 nm nm. Strong coupling can be observed from t = 104 nm and designed structure achieves almost 100 % absorbance for t = 155 nm. The resonance peak position shows a longer wavelength shift with an increase in the grating thickness. After optimizing grating width (W) and thickness (t), we studied the effect of grating period on the reflectance dip and resonance wavelength. We can observe that resonance peak wavelength significantly depends on the grating period and a continuous red shift in resonance wavelength can be observed, Fig. 2 (e)(f).

B. Spatial Distribution for Electric and Magnetic Field at Optimized Grating

In the previous section, we designed a 1D plasmonic grating and numerically optimized its geometric parameters as

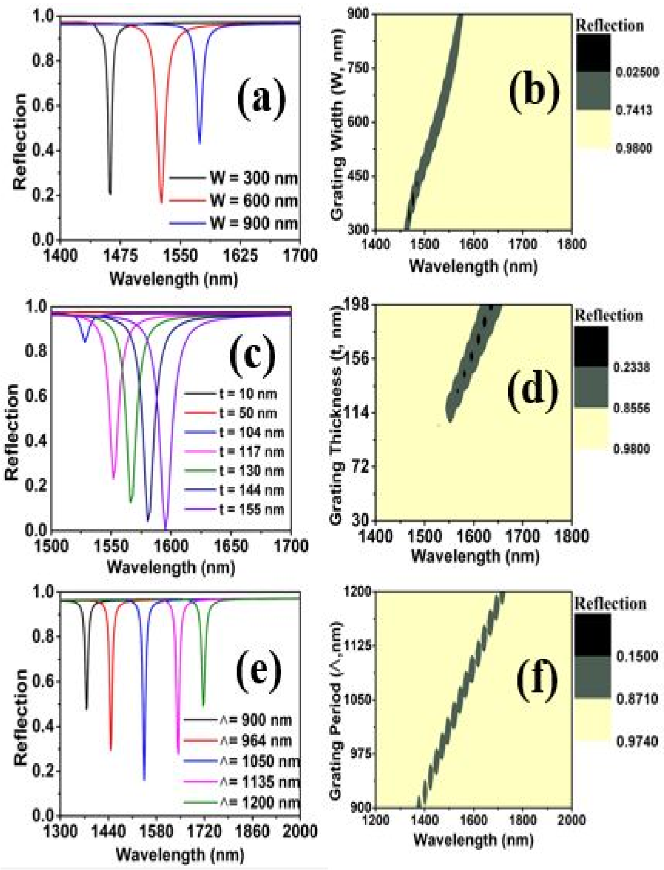

Fig. 2. (a, b) Reflection spectra for varying grating width *W*, keeping grating period = 1060 nm and grating thickness *t* = 125 nm fixed. (c), (d) Reflection spectra for varying grating thickness *t*, keeping grating period Λ = 1060 nm and grating width *W* = 600 nm fixed. (e), (f) Reflection spectra for varying grating period Λ, keeping grating thickness t = 125 nm and grating width *W* = 600 nm fixed.

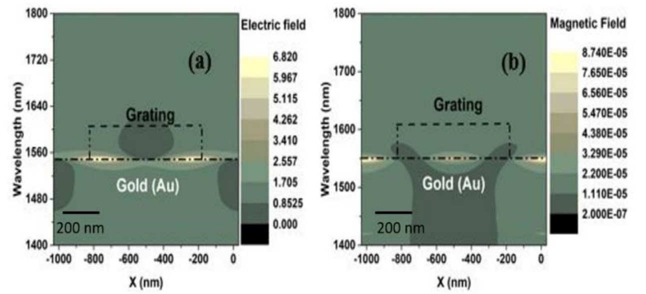

Fig. 3. (a) Electric and (b) magnetic field distribution from power monitor above for broadband with following parameters: grating period Λ = 1060 nm, grating width W = 600 nm and grating thickness t = 135 nm.

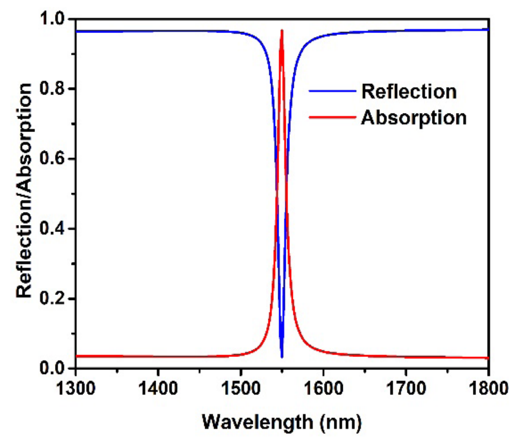

Fig. 4. Reflection and absorption of the proposed structure using following parameters: grating period Λ = 1060 nm, Λ = 1060 nm, grating width *W* = 700 nm and grating thickness t = 135 nm.

W = 600 nm, t = 135 nm and Λ = 1060 nm to get maximum FOM for plasmonic mode. The simulation results, obtained in the previous section, suggest that the designed structure can be realized for broadband tuning of resonance peak in the NIR region. by adjusting its geometric parameters. Understanding the spatial distribution of spectral electric and magnetic field, at resonance wavelength, for optimized plasmonic structure is highly important. Field distribution corresponding to a power monitor above FDTD simulation region is shown in Fig. 3 (a) and (b). When a X polarized electromagnetic wave propagates in the y direction the electric field distribution of x component dominates. The electric field distribution shows the excitement of surface plasmon resonance at resonance wavelength. It can be seen that maximum field confinement is around at 1500 nm, which is resonance wavelength for the optimized structure.

For an optimized structure, we also put a transmission monitor below the silicon nitride substrate to calculate absorption using A =1-T-R. Fig. 4 presents reflection and calculated absorption spectra of the proposed structure, under normal incidence, with a grating period of Λ = 1060 nm, W = 700 nm and t = 135 nm on 300 nm gold film over silicon nitride substrate. The refractive index of dielectric substrate Si_3N_4 is fixed around 2.05. Due to large thickness of gold layer the structure has almost negligible transmission in the studied spectral range, therefore 1-R can be safely considered as absorbance for the structure. Due to the thickness of gold, the transmission characteristic of the structure is perfectly suppressed by the structure. So, the absorption can be calculated using $A = 1\text{-}R$, Where R and T are reflection and transmission respectively. To excite SPP mode at 1550 nm and considering narrow line width, lowest reflection and strong coupling, we fix our grating period at Λ = 1060 nm, W = 700 nm and t = 135 nm for all further calculations.

Fig. 4 is showing the normal incident reflection and absorption spectra for the proposed structure with a grating period of Λ = 1060 nm, W = 700 nm and t = 135 nm thick BAF-10 grating on 300 nm gold film over silicon nitride substrate. The refractive index of dielectric substrate Si_3N_4 is fixed around 2.05.

It can be observed from the curve that there is only one sharp rejection band at λ_0 = 1550 nm, which is known as resonance wavelength. The sharp rejection, or dip, indicates the coupling of surface plasmon modes. It can also be observed that the structure has narrow bandwidth (FWHM of 2.5 nm) resonance absorption with nearly unit peak absorbance. The designed structure can be also used to selectively excite a vibrational mode of any biomolecule in water or other solvent to get its SEIRA signal without exciting mode of water molecules.

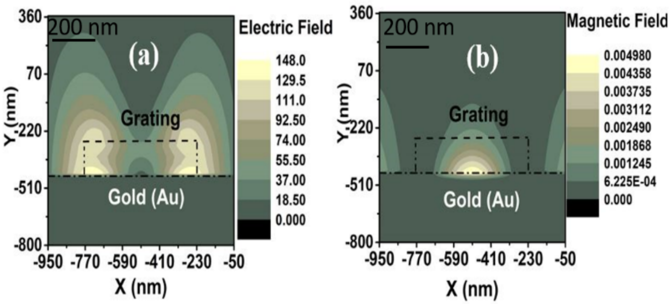

Fig. 5. (a) Electrical field distribution at resonance wavelength $\lambda_0 =$ 1550 nm. (b) Magnetic field distribution at resonance wavelength $\lambda_0 =$ 1550 nm, using following parameters: grating period Λ = 1060 nm, grating width W = 700 nm and grating thickness t = 135 nm.

Spatial distribution of electric and magnetic fields at resonance wavelength is important to understand the spatial localization of power. Therefore, field distribution corresponding to a resonance wavelength $\lambda_0 = 1550$ nm has been calculated and shown in Fig. 5(a) and (b). The black dashed line shows a unit cell of optimized grating structure. The field strength is represented by color code. From Fig. 5, it can be observed that the electric field resonance mode is localized at the interfaces made by lower two corners of BAF grating and gold film, while magnetic resonance is localized at the center of BAF grating and gold film interface. This is due to the strong coupling of surface plasmon mode at resonance wavelength. Enhancement in the electric field intensity at resonance wavelength or frequency is the fundamental point for biosensing applications.

C. Sensitivity to Change in Ambience Refractive Index and Glucose Concentration Detection

After optimizing geometrical parameters and observing field distribution, we will present the response of the proposed structure for the detection of glucose concentration in a water. The reflection response of designed and optimized structure is simulated for different glucose concentration in the range 0 g/100 ml (pure water) to 30 g/ 100ml. Refractometric method is used for determination of sugar percentage in a water. This method basically determines the refractive index of known glucose concentration to make a line-of-calibration. The obtained line-of-calibration can be used to determine concentration of unknown glucose concentration from its measured refractive index. The following expression calculates the refractive index of an aqueous solution of glucose:

$$n = n_W + aC \tag{7}$$

here n_W stands for the refractive index of water at 25°C, $a = 0.00143$ is constant, and C is sugar concentration in g/100 ml. First equation (7) is used to determine refractive index of glucose concentration in the range of 0 to 30 g in 100 ml of water, and then obtained index is used to simulate corresponding spectral response of designed structure. Refractive index of ambient, in the grooves and top of the grating, is varied numerically following the equation (7) to determine reflectance response of the structure for different concentration of glucose in the water. According to LC equivalent circuit model [38], an increase in the refractive index and hence permittivity between two ridges of the grating increases its capacitance that attributes longer wavelength shift in the resonance wavelength. Fig 6 (a) shows spectral reflectance from an optimized plasmonic structure (Λ = 1060 nm, W = 700 nm and t= 135 nm) at different glucose concentration. An increase in the glucose concentration causes shift in the resonance wavelength towards longer wavelength with decrease in dip-strength. Fig 6 (b) shows variation in refractive index and resonance wavelength with glucose concentration. Fig. 6 (b) helps us to choose glucose concentration and its corresponding resonance wavelength and refractive index. We characterize the proposed structure by calculating its sensitivity, FWHM, quality factor, dip strength and FOM. Sensitivity is the slope of fig. 6 (b), higher the slope means better sensitivity.

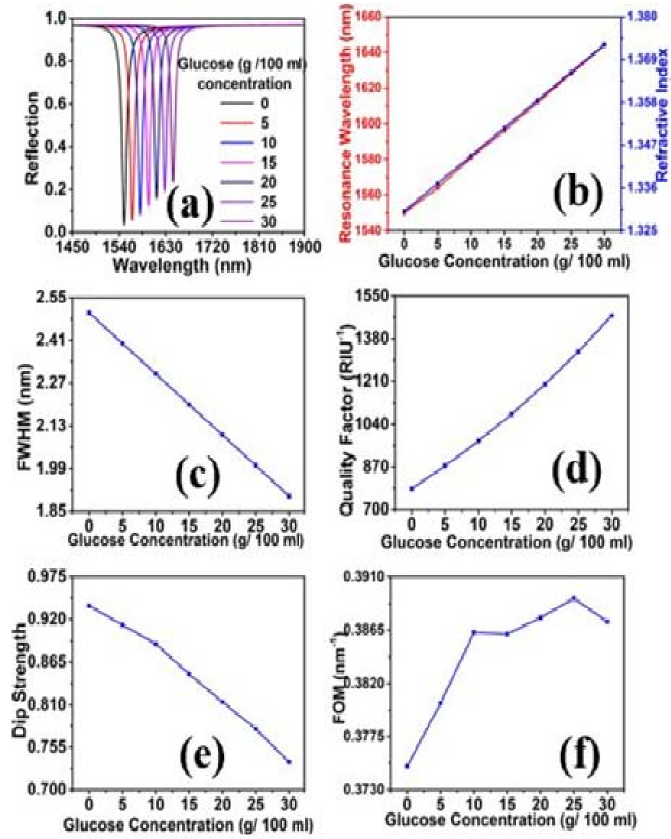

Fig. 6. (a) Reflection with varying ambient refractive index; (b) Glucose concentration versus refractive index (left) and corresponding resonance wavelength (right), (c) FWHM (d) Quality factor (e) Dip strength and (f) FOM using following parameters: grating period Λ = 1060 nm, grating width W = 700 nm and grating thickness t = 135 nm.

The bandwidth (FHWM) of resonance peak shows accuracy, so better accuracy corresponds to narrower SPR peak. Dip strength is calculated by subtracting minimum reflectivity from maximum. Dip strength should be large enough for clear observation of peak. Quality factor and FOM are calculated using equations 4 and 5 and presented in figure 6 (d) and (f) respectively. The calculated sensitivity and quality factor of the designed plasmonic sensor for the glucose detection are $\sim$ 2300 nm/RIU and $\sim$1500 RIU^{-1} respectively with a narrow bandwidth of 2.5 nm. From these simulation results, we believe that performance metrices of plasmonic sensors that will be fabricated following the designed structure would be highly satisfactory in the detection of low concentration of blood glucose.

IV. Conclusion

In summary, we designed an easy to fabricate plasmonic sensor with high sensitivity and high-quality factor in infrared for biomolecular detection. The designed structure is based on 1-D grating pattern of barium flint glass on gold thin film deposited on silicon nitride substrate. The effects of different geometric parameters such as grating width, thickness of gold film and grating period on the characteristics of resonance absorption have been thoroughly investigated to optimized plasmonic structure. The grating parameters are found fine reliable knobs to tune resonance peak position in broad spectral range in infrared. This capability of designed structure along with narrow spectral bandwidth make it perfect surface-enhanced-infrared absorption (SEIRA) substrate to selectively excite vibrational modes of target biomolecule in solution without effecting the vibrational mode of matrix molecule (such as water) for single molecule detection. The performance of designed and optimized structure is tested for the detection of glucose concentration in water with sensitivity and quality factor as high as $\sim$ 2300 nm/RIU and $\sim$1500 RIU^{-1} respectively with spectral bandwidth as narrow as 2.5 nm. Furthermore, due to having a very narrow rejection band, proposed structure can also be used as a narrow band-rejection filter in the infrared. The aforementioned benefits, especially high FOM and sensitivity, show that the proposed structure could be a reliable candidate for bio sensing applications, gas detection, and bio-medical diagnosis. In the future, we will fabricate designed plasmonic structure for realization of low cost but high value narrowband rejection filters, SEIRA substrates, and plasmonic sensors.

References

[1] S. A. Maier, *Plasmonics: Fundamentals and Applications*. New York, NY, USA: Springer, 2007, doi: 10.1007/0-387-37825-1.

[2] U. Fano, "The theory of anomalous diffraction gratings and of quasi-stationary waves on metallic surfaces (sommerfeld's waves)," *J. Opt. Soc. Amer.*, vol. 31, no. 3, pp. 213–222, Mar. 1941.

[3] E. Kretschmann and H. Raether, "Notizen: Radiative decay of non radiative surface plasmons excited by light," *Zeitschrift Naturforschung A*, vol. 23, no. 12, pp. 2135–2136, Dec. 1968.

[4] B. Liedberg, C. Nylander, and I. Lunström, "Surface plasmon resonance for gas detection and biosensing," *Sens. Actuators*, vol. 4, pp. 299–304, Jan. 1983.

[5] B. Wang, S. C. Singh, H. Lu, and C. Guo, "Design of aluminum bowtie nanoantenna array with geometrical control to tune LSPR from UV to near-IR for optical sensing," *Plasmonics*, to be published, doi: 10.1007/s11468-019-01071-z.

[6] C. Yao, S. C. Singh, M. ElKabbash, J. Zhang, H. Lu, and C. Guo, "Quasi-rhombus metasurfaces as multimode interference couplers for controlling the propagation of modes in dielectric-loaded waveguides," *Opt. Lett.*, vol. 44, no. 7, pp. 1654–1657, 2019.

[7] J. Zhang, M. ElKabbash, R. Wei, S. C. Singh, B. Lam, and C. Guo, "Plasmonic metasurfaces with 42.3% transmission efficiency in the visible," *Light: Sci. Appl.*, vol. 8, no. 1, pp. 53–66, 2019.

[8] D. Chu, S. C. Singh, Z. Zhan, X. Sun, J. A. Duan, and C. Guo, "Creation of enhanced transmission for clear and frosted glass through facile surface texturing," *Opt. Mater. Express*, vol. 9, no. 7, pp. 2946–2954, 2019.

[9] A. Ahmadivand, B. Gerislioglu, R. Ahuja, and Y. K. Mishra, "Terahertz plasmonics: The rise of toroidal metadevices towards immunobiosensings," *Mater. Today*, to be published, doi: 10.1016/j.mattod.2019.08.002.

[10] G. Chen, K. J. Lee, and R. Magnusson, "Periodic photonic filters: Theory and experiment," *Opt. Eng.*, vol. 55, no. 3, Mar. 2016, Art. no. 037108.

[11] D. W. Peters *et al.*, "Demonstration of polarization-independent resonant subwavelength grating filter arrays," *Opt. Lett.*, vol. 35, no. 19, pp. 3201–3203, Oct. 2010.

[12] T. Kondo, S. Ura, and R. Magnusson, "Design of guided-mode resonance mirrors for short laser cavities," *J. Opt. Soc. Amer. A, Opt. Image Sci.*, vol. 32, no. 8, pp. 1454–1458, Aug. 2015.

[13] S. S. Wang and R. Magnusson, "Theory and applications of guided-mode resonance filters," *Appl. Opt.*, vol. 32, no. 14, pp. 2606–2613, May 1993.

[14] L. Lu *et al.*, "A portable optical fiber SPR temperature sensor based on a smart-phone," *Opt. Express*, vol. 27, no. 18, pp. 25420–25427, Sep. 2019.

[15] A. Sharma and C. Marques, "Design and performance perspectives on fiber optic sensors with plasmonic nanostructures and gratings: A review," *IEEE Sensors J.*, vol. 19, no. 17, pp. 7168–7178, Sep. 2019, doi: 10.1109/JSEN.2019.2915274.

[16] M. Lobry *et al.*, "Non-enzymatic D-glucose plasmonic optical fiber grating biosensor," *Biosensors Bioelectron.*, vol. 142, Oct. 2019, Art. no. 111506.

[17] X. Fu, K. Yi, J. Shao, and Z. Fan, "Nonpolarizing guided-mode resonance filter," *Opt. Lett.*, vol. 34, no. 2, pp. 124–126, Jan. 2009.

[18] S. Tibuleac and R. Magnusson, "Reflection and transmission guided-mode resonance filters," *J. Opt. Soc. Amer. A, Opt. Image Sci.*, vol. 14, no. 7, pp. 1617–1626, Jul. 1997.

[19] W. Liu, Z. Lai, H. Guo, and Y. Liu, "Guided-mode resonance filters with shallow grating," *Opt. Lett.*, vol. 35, no. 6, pp. 865–867, Mar. 2010.

[20] X. Liu, G. Liu, G. Fu, M. Liu, and Z. Liu, "Monochromatic filter with multiple manipulation approaches by the layered all-dielectric patch array," *Nanotechnology*, vol. 27, no. 12, Mar. 2016, Art. no. 125202.

[21] X. Xiong, S.-C. Jiang, Y.-H. Hu, R.-W. Peng, and M. Wang, "Structured metal film as a perfect absorber," *Adv. Mater.*, vol. 25, no. 29, pp. 3994–4000, Aug. 2013.

[22] J. Wu, C. Zhou, J. Yu, H. Cao, S. Li, and W. Jia, "TE polarization selective absorber based on metal-dielectric grating structure for infrared frequencies," *Opt. Commun.*, vol. 329, no. 20, pp. 38–43, Oct. 2014.

[23] T. Wu, Y. Liu, Z. Yu, Y. Peng, C. Shu, and H. Ye, "The sensing characteristics of plasmonic waveguide with a ring resonator," *Opt. Express*, vol. 22, no. 7, p. 7669, Apr. 2014.

[24] C. Sabah, F. Dincer, M. Karaaslan, E. Unal, O. Akgol, and E. Demirel, "Perfect metamaterial absorber with polarization and incident angle independencies based on ring and cross-wire resonators for shielding and a sensor application," *Opt. Commun.*, vol. 322, pp. 137–142, Jul. 2014.

[25] J. Le Perchec, P. Quémerais, A. Barbara, and T. López-Ríos, "Why metallic surfaces with grooves a few nanometers deep and wide may strongly absorb visible light," *Phys. Rev. Lett.*, vol. 100, no. 6, 2008, Art. no. 066408.

[26] S. Luo, J. Zhao, D. Zuo, and X. Wang, "Perfect narrow band absorber for sensing applications," *Opt. Express*, vol. 24, no. 9, pp. 9288–9294, May 2016.

[27] X. Lu, R. Wan, F. Liu, and T. Zhang, "High-sensitivity plasmonic sensor based on perfect absorber with metallic nanoring structures," *J. Mod. Opt.*, vol. 63, no. 2, pp. 177–183, Jan. 2016.

[28] Z.-Q. Liu *et al.*, "λ^3/20000 plasmonic nanocavities with multispectral ultra-narrowband absorption for high-quality sensing," *Appl. Phys. Lett.*, vol. 104, no. 8, Feb. 2014, Art. no. 081116.

[29] G. Liu *et al.*, "Multi-band high refractive index susceptibility of plasmonic structures with network-type metasurface," *Plasmonics*, vol. 11, no. 2, pp. 677–682, Apr. 2016.

[30] M. Baqir, M. Ghasemi, P. Choudhury, and B. Majlis, "Design and analysis of nanostructured subwavelength metamaterial absorber operating in the UV and visible spectral range," *J. Electromagn. Waves Appl.*, vol. 29, no. 18, pp. 2408–2419, Dec. 2015.

[31] N. Liu, M. Mesch, T. Weiss, M. Hentschel, and H. Giessen, "Infrared perfect absorber and its application as plasmonic sensor," *Nano Lett.*, vol. 10, no. 7, pp. 2342–2348, Jul. 2010.

[32] Y. Cui *et al.*, "Ultrabroadband light absorption by a sawtooth anisotropic metamaterial slab," *Nano Lett.*, vol. 12, no. 3, pp. 1443–1447, Mar. 2012.

[33] M. K. Hedayati *et al.*, "Design of a perfect black absorber at visible frequencies using plasmonic metamaterials," *Adv. Mater.*, vol. 23, no. 45, pp. 5410–5414, Dec. 2011.

[34] Y. Cui *et al.*, "A thin film broadband absorber based on multi-sized nanoantennas," *Appl. Phys. Lett.*, vol. 99, no. 25, Dec. 2011, Art. no. 253101.

[35] Y. Shen *et al.*, "Plasmonic gold mushroom arrays with refractive index sensing figures of merit approaching the theoretical limit," *Nature Commun.*, vol. 4, p. 2381, Aug. 2013.

[36] X. Lu, L. Zhang, and T. Zhang, "Nanoslit-microcavity-based narrow band absorber for sensing applications," *Opt. Express*, vol. 23, no. 16, pp. 20715–20720, Aug. 2015.

[37] Lumerical Inc. *Lumerical Solutions*. Accessed: Sep. 2019. [Online]. Available: https://www.lumerical.com/products/fdtd-solutions/

[38] E. D. Palik, *Handbook of Optical Constants of Solids II*, vol. 1, no. 1. Boston, MA, USA: Academic, 1991, pp. 77–135.

[39] D. Wu *et al.*, "Ultra-narrow band perfect absorber and its application as plasmonic sensor in the visible region," *Nanosc. Res. Lett.*, vol. 12, no. 1, p. 427, 2017, doi: 10.1186/s11671-017-2203-9.

Sandeep Kumar Chamoli received the master's degree from the Indian Institute of Technology Roorkee (IITR), in 2017. He is currently pursuing the Ph.D. degree with the Guo China-US Photonics Laboratory, the Collaborative Laboratory between CIOMP, CAS, and the University of Rochester, USA. After masters and before joining Guo Laboratory, he was the part of Monash University from October 2017 to June 2018 as a Research Assistant and working on Single Pixel Imaging and Laser Sensing. He is also working on Plasmonics and Metamaterials. He is awardee of Prestigious CAS-TWAS Fellowship for International Doctorate Student.

Subhash Chandra Singh was an IRCSET EMPOWER Postdoctoral Research Fellow at Dublin City University, Ireland, for two years and a DST-SERB Young Scientist at the University of Allahabad, India, for three years. He is currently an Associate Professor with the Guo's Photonics Laboratory, CIOMP, and a Visiting Scientist with The Institute of Optics, University of Rochester, New York. Dr. Singh has more than ten years of postdoctoral research experience in the field of laser–matter interaction, plasma and nanomaterial processing, and spectroscopy of atoms and molecules. He has published more than 80 research articles in high impact factor refereed journals and conference proceedings. His current research interests include laser–matter interaction, strong field multi-photon ionization, plasmonic, photonics, and energy harvesting devices. He is also advising two research students at CIOMP in the area of plasmonic waveguides and plasmonic nanolasers.

Chunlei Guo received the Ph.D. degree in physics from the University of Connecticut in 1999 and was later named one of the University's 40 Under 40 Outstanding Alumni.

From 1999 to 2011, he was a Postdoctoral Associate with the Los Alamos National Laboratory, where his work was awarded the Postdoctoral Publication Prize in Experimental Sciences. Since 2001, he has been joined the faculty of the University of Rochester. He is the Director of the Guo China-US Photonics Laboratory and also a Full Professor with The Institute of Optics, University of Rochester. His research interests focus on laser–matter interactions at high intensities, nano-photonics, femtosecond laser surface nano and microstructure, and surface plasmonics. He and his coworkers invented the so-called black and colored metals, which have a broad range of technological applications and have been covered extensively by the media.

Prof. Guo is an elected Fellow for American Physical Society, Optical Society of America, and International Academy of Photonics & Laser Engineering. He serves as an Editor and on editorial boards for a number of scientific journals and is the past Chair of Short-Wavelength and High-Field Physics Group in the Optical Society of America.